Electronic Supplementary Information for

Superior performance and stability of anion exchange membrane water electrolysis: pH-controlled copper cobalt oxide nanoparticle for oxygen evolution reaction

Myeong Je Jang‡[ab], Juchan Yang‡[a], Jongmin Lee‡[c], Yoo Sei Park[ad], Jaehoon Jeong [a], Seong Min Park[ad], Jae-Yeop Jeong[ad], Yadong Yin[e], Min-Ho Seo*[c], Sung Mook Choi*[a], Kyu Hwan Lee*[ab]

[a] Surface Technology Department, Korea Institute of Materials Science, 797 Changwon-Daero, Sungsan-gu, Changwon, 51508, Republic of Korea

[b] Advanced Materials Engineering, Korea University of Science and Technology (UST), 217 Gajeong-ro, Yuseong-gu, Daejeon, 34113, Republic of Korea

[c] Buan Fuel Cell Center, New and Renewable Energy Institute, Korea Institute of Energy Research (KIER), 20-41, Sinjaesaengeneogi-ro, Haseo-myeon, Buan-gun, 56332, Republic of Korea

[d] Department of Materials Science and Engineering, Pusan National University, Busan, 46241, Republic of Korea

[e] Department of Chemistry, Center for Catalysis, University of California Riverside, Riverside, California 92521, United States

Table S1. The atomic percentage of Cu and Co from TEM-EDS, XPS and ICP-MS.

Catalysts	TEM-EDS Cu (at.%)	TEM-EDS Co (at.%)	XPS Cu (at.%)	XPS Co (at.%)	ICP-MS Cu (at.%)	ICP-MS Co (at.%)
CCO-8	85.8	14.2	64.3	35.7	74.0	26.0
CCO-9	74	26	-	-		
CCO-9.5	25.2	74.8	25.8	74.2	47.7	52.3
CCO-11	16.2	83.8	16.18	83.82	4.5	95.5

Table S2. Comparison of the OER activity of Co-based electrocatalysts in alkaline electrolytes.

Electrocatalyst	**Catalyst loading (mg cm^{-2})**	**Substrate**	**Electrolyte**	**Overpotential at 10 mA cm^{-2} (mV)**	**Tafel slope (mV dec^{-1})**	**Ref.**
NiCo-r	0.285	GCE	1 M KOH	320	30	[1]
CoOx-4h	0.5	GCE	1 M KOH	306	65	[2]
$Co_3O_4/NiCo_2O_4$ DSNCs	1	Ni foam	1 M KOH	340	88	[3]
Co_3O_4 nanowire	0.136	GCE	1 M KOH	400	72	[4]
CoO hexagrams	0.28	GCE	1 M KOH	269	64.4	[5]
Ni-Co oxide	Not given	FTO	1 M NaOH	340	51	[6]
Ni–Co oxide cages	Not given	GCE	1 M KOH	380	50	[7]
$Au@CoFeO_x$	Not given	GCE	1 M KOH	328	58	[8]
Au/mCo_3O_4	Not given	GCE	0.1 M KOH	440	46	[9]
$Cu_{0.5}Co_{2.5}O_4$	0.5	GCE	1 M KOH	285	79.2	This work

Table S3. Comparison of the AEMWE reported performance with OER catalyst, HER catalyst, AEM, binder, electrolyte and temperature.

OER catalyst Loading (mg cm^{-2})	**HER catalyst Loading (mg cm^{-2})**	**AEM**	**Binder**	**Electrolyte**	**Temperature [°C]**	**Cell performance current density [mA cm^{-2}]/voltage [V]**	**Ref.**
$Cu_{0.7}Co_{2.3}O_4$ nanopowder (3)	Ni nanopowder (2)	Cranfield-membrane	Quaternized Poly(DMAEMA-co-TFEMA-co-BMA) (QPDTB) ionomer	0.1 M KOH	55 (Bath)	150 / 2.0	[10]
$Cu_{0.7}Co_{2.3}O_4$ nanopowder (3)	Ni nanopowder (2)	qPVB/OH^-	qPVB/Cl ionomer	1 M KOH	55 (Bath)	100 / 2.0	[11]
$CuCoO_x$ (36)	Ni-CeO_2-La_2O_3/C (7.4)	A201, Tokuyama	PTFE	1 M KOH	55 (Bath)	450 / 1.8	[12]
Ni–Fe nanopowder (Not given)	Ni-Mo (40)	Quaternary ammonia polysulfone (xQAPS)	xQAPS	D.I.	70 (Bath)	250 / 1.8	[13]
$Li_{0.21}Co_{2.79}O_4$ (2.5)	Ni nanopowder (2)	Cranfield-membrane	QPDTB ionomer	D.I.	45 (Not given)	245 / 2.0	[14]
$Ce_{0.2}MnFe_{1.8}O_4$ (3.5)	Ni nanopowder (3.5)	Fumasep® FAA-3-PK-130	AEM dissolved in dimethyl sulfoxide	D.I.	25 (Not given)	250 / 1.8	[15]
$Cu_xCo_{3-x}O_4$ nanoparticles (3)	Pt/C (1)	Cranfield-membrane	Not given	1 M KOH	25 (Bath)	1000 / 1.8	[16]
IrO_2 (2.9)	Pt black (3.2)	A201, Tokuyama	AS-4, Tokuyama	1 M KOH	50 (Cell)	399 / 1.8	[17]
IrO_2 (4)	Pt/C (0.4)	Fumasep® FAA-3-50, Fumatech	FAA-3-Br, Fumatech	1 M KOH	50 (Cell)	1150 / 1.8	[18]
IrO_2 (Not given)	Pt/C (Not given)	A201, Tokuyama	PTFE	0.5 M KOH	50 (Not given)	1070 / 1.8	[19]
$Cu_{0.5}Co_{2.5}O_4$ (10)	Pt/C (1)	X37-50 T, Dioxide Materials	PTFE	1 M KOH	50 (Bath) 45 (Cell)	1300 / 1.8	This work

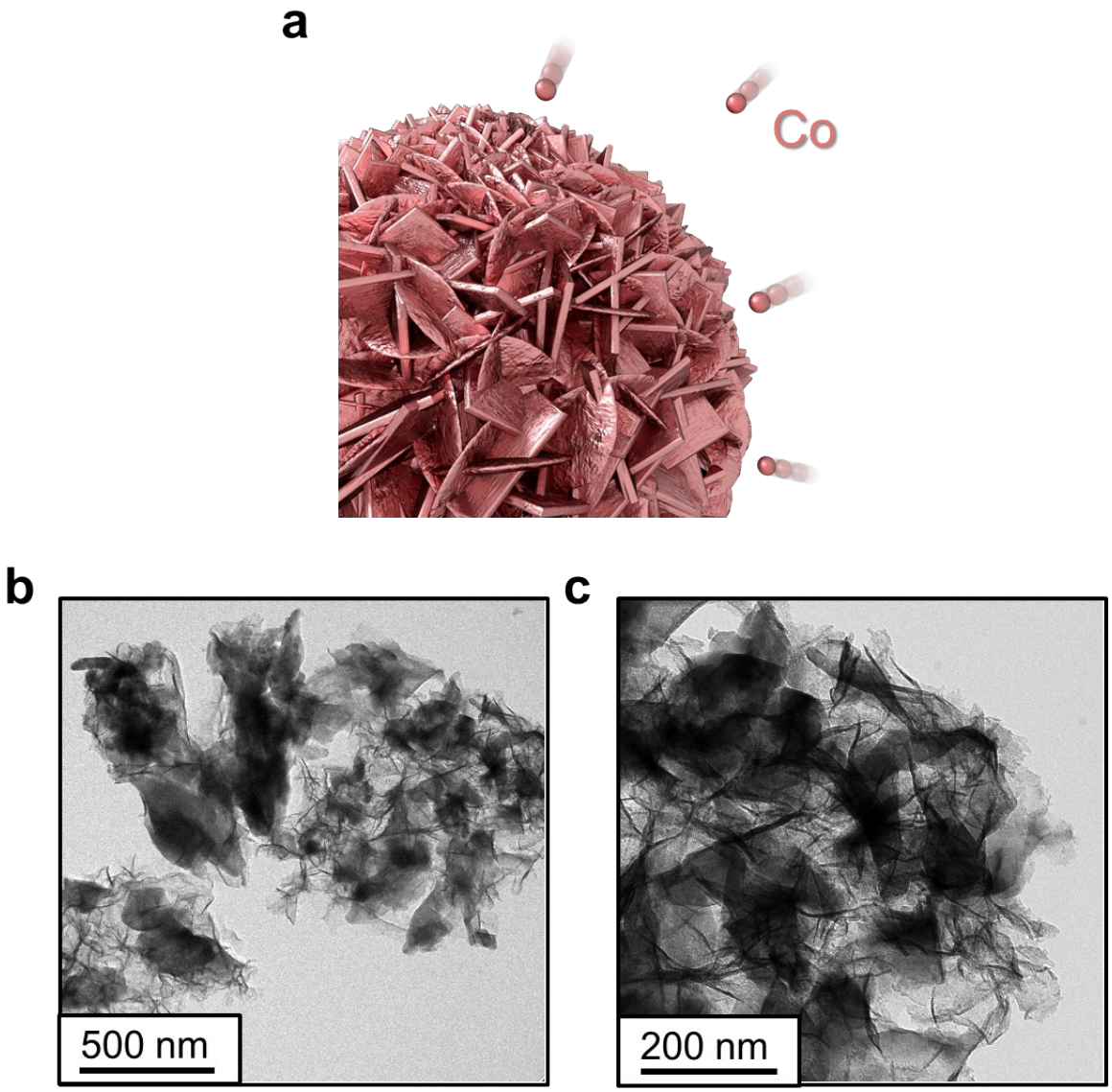

Fig. S1. (a) The schematic diagram showing the formation of Cu-Co hydroxide nanowalls. TEM image of CCO-9.5 with magnification (b)×12,000 and (c)×30,000.

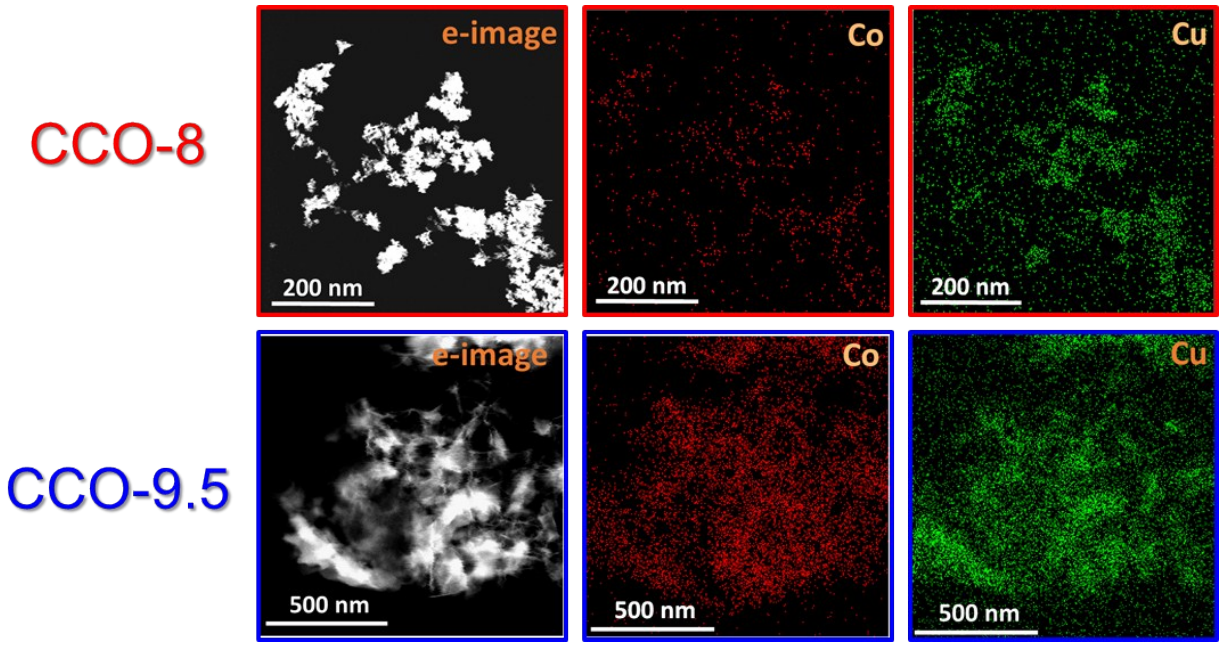

Fig. S2. Elemental mapping of the electron image, Co and Cu of the CCO-8 and CCO-9.5.

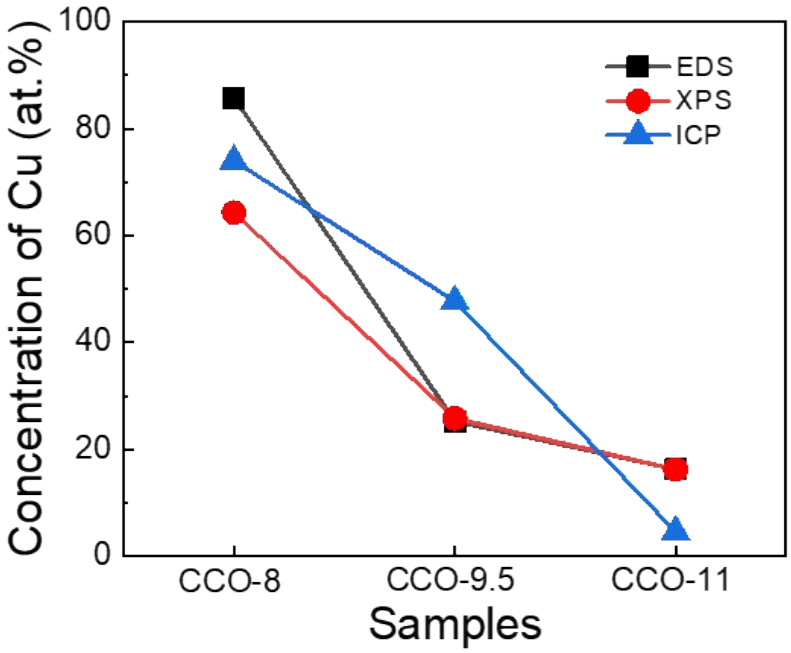

Fig. S3. The atomic percentage of Cu in CCO-8, CCO-9.5 and CCO-11 electrocatalyst from TEM-EDS, XPS and ICP-MS.

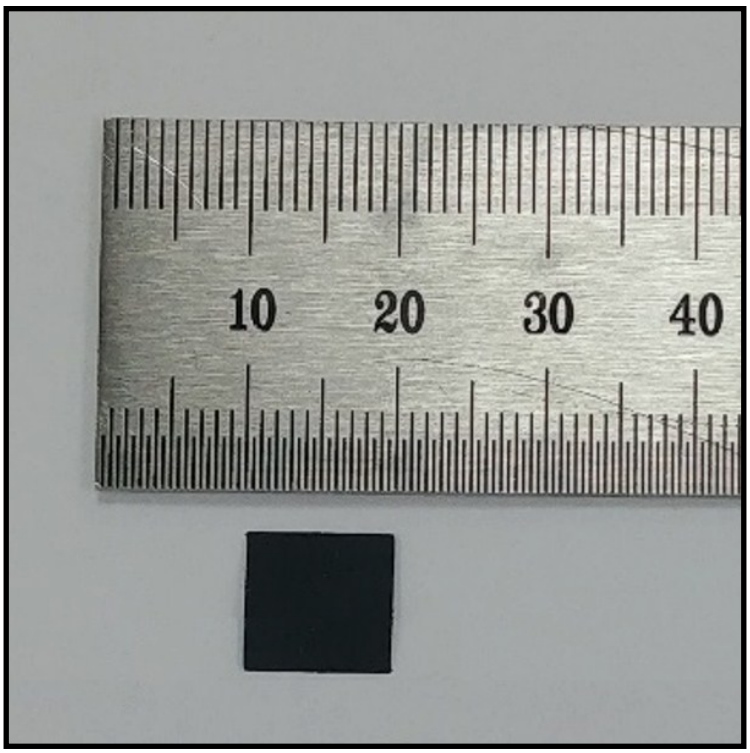

Fig. S4. Photograph of the CCO-11 (1 cm^2) on Ni foam electrode by hot pressing.

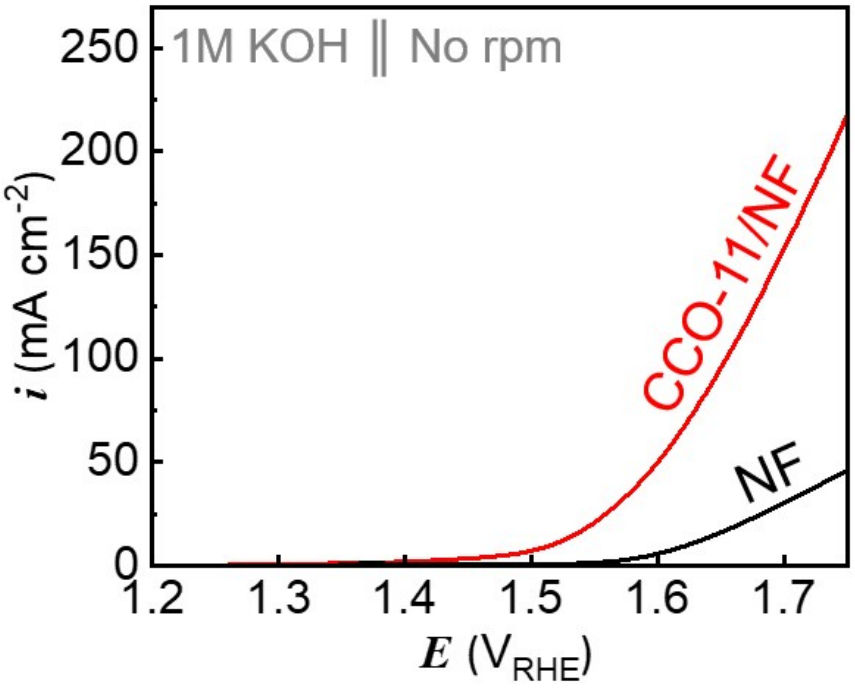

Fig. S5.. The half cell polarization curves of CCO-11/NF (10 mg cm^{-2}) and pure Ni foam (NF) in 1 M KOH.

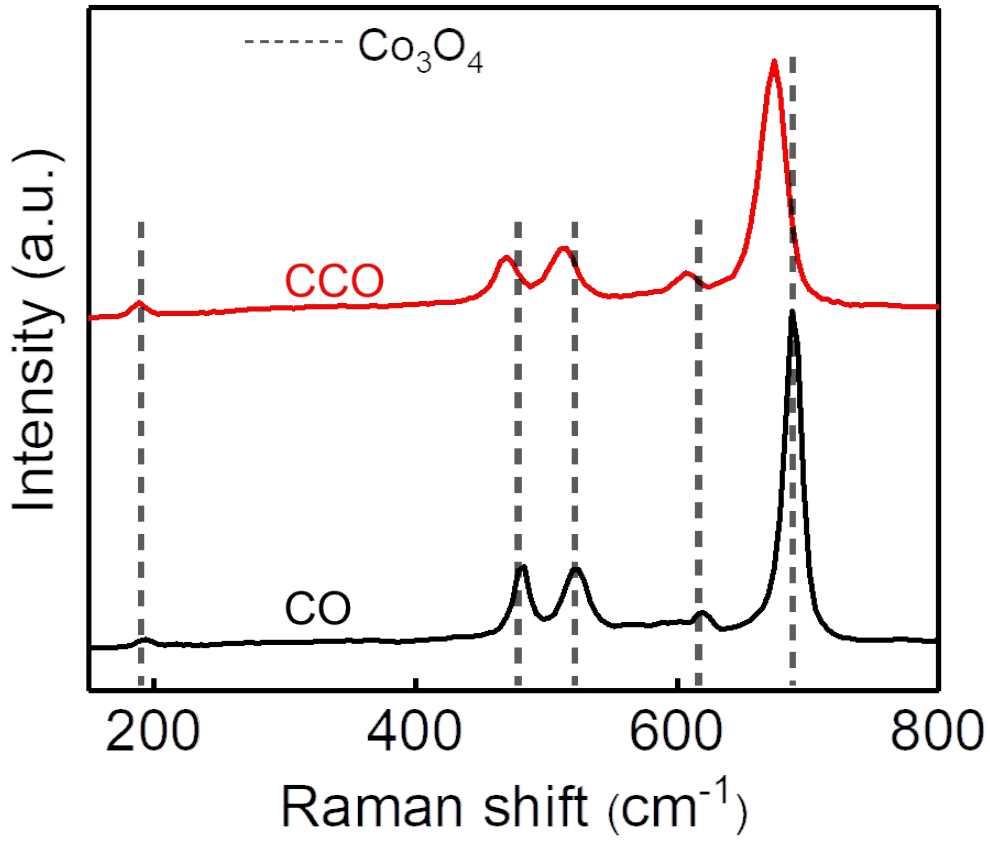

Fig. S6. The Raman spectra of CCO and CO.

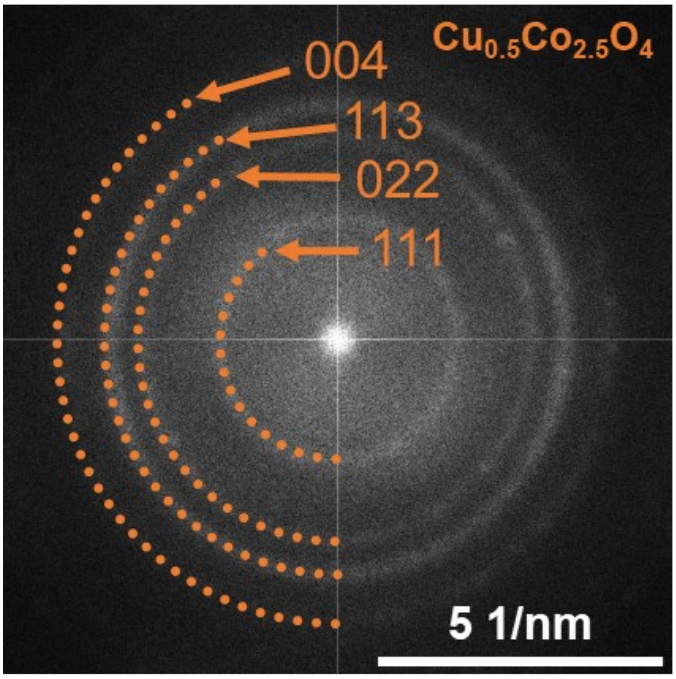

Fig. S7. The SAED pattern of the CCO-11 catalyst.

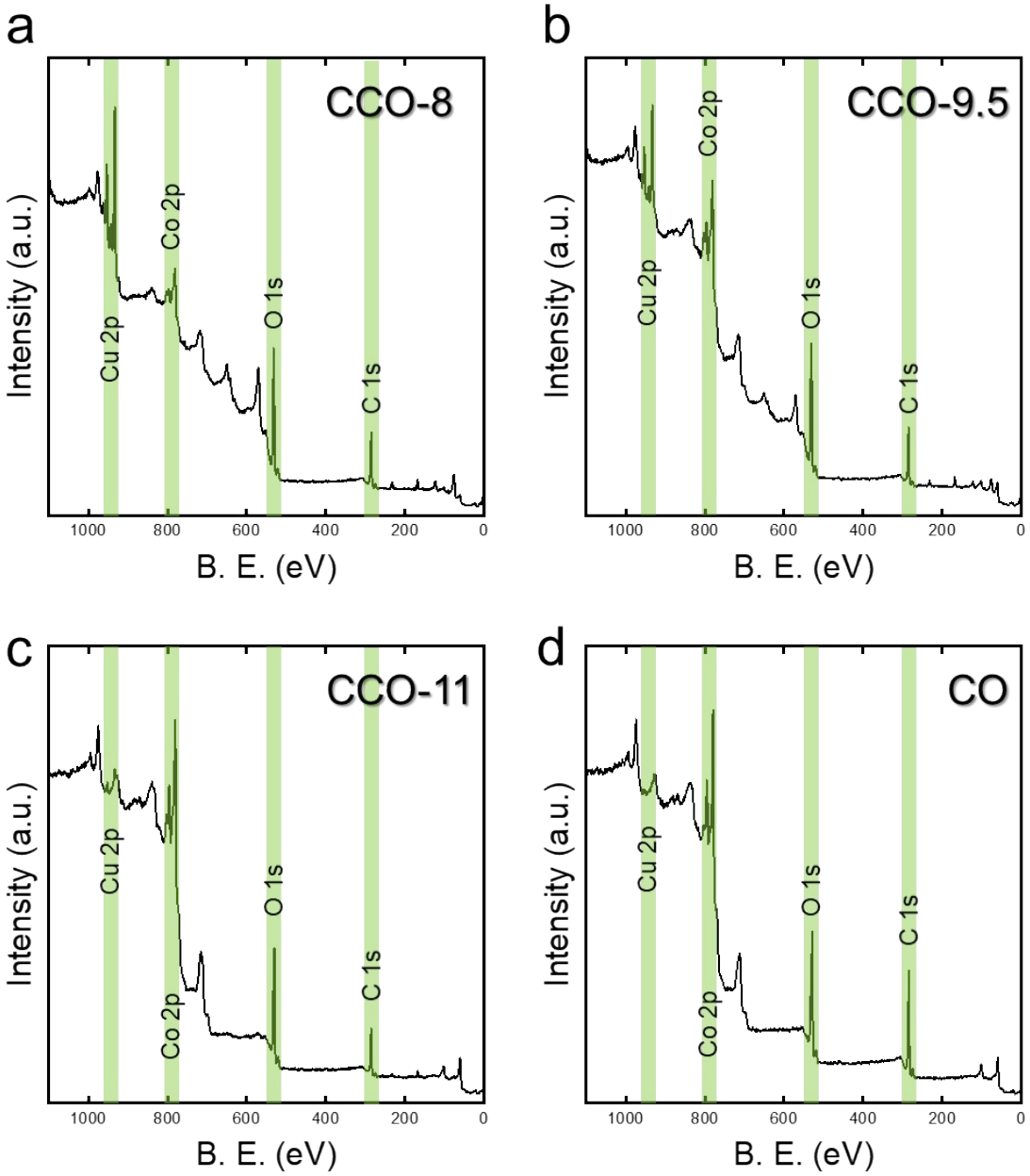

Fig. S8. XPS survey spectra of CCO-8, CCO-9.5, CCO-11 and CO.

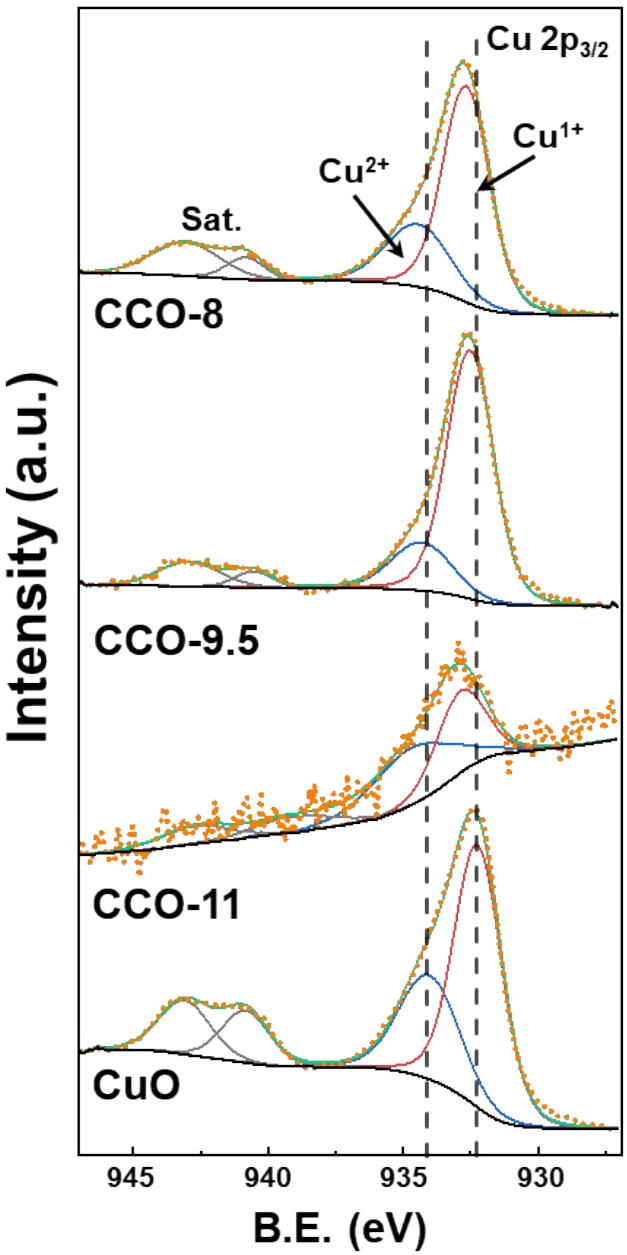

Fig. S9. XPS spectra of Cu 2p3/2 of the CuO, CCO-8, CCO-9.5 and CCO-11.

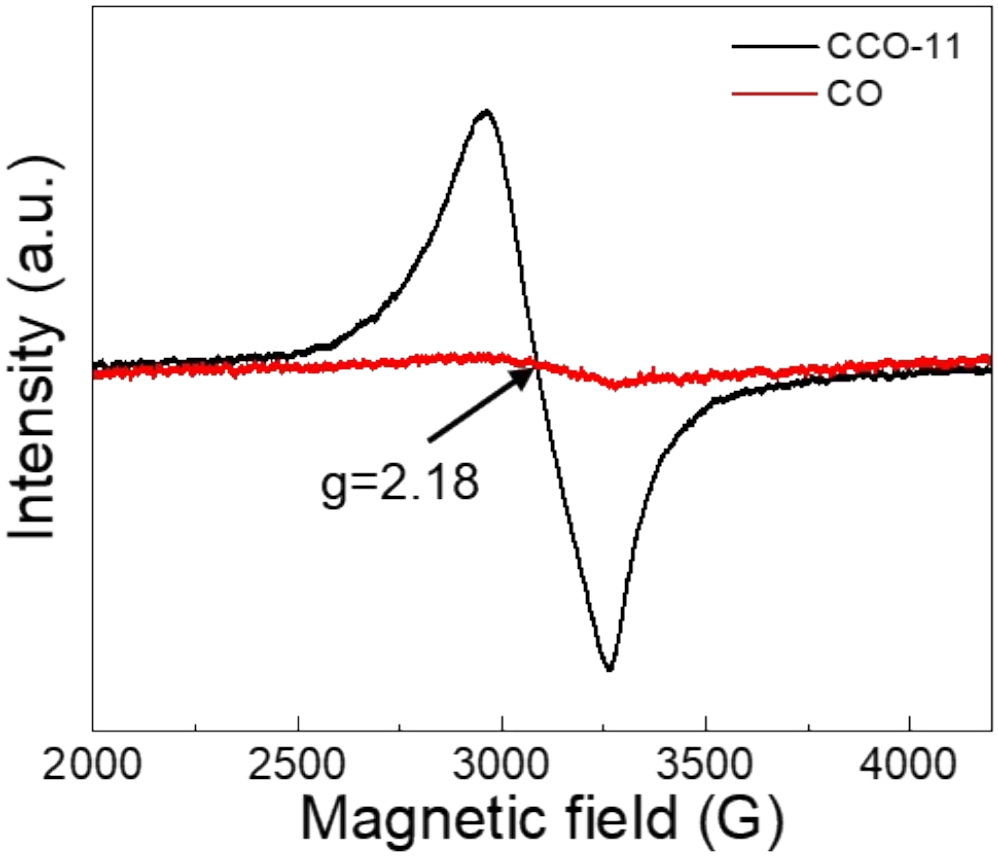

Fig. S10. Room-temperature EPR spectra of CCO-11 and CO.

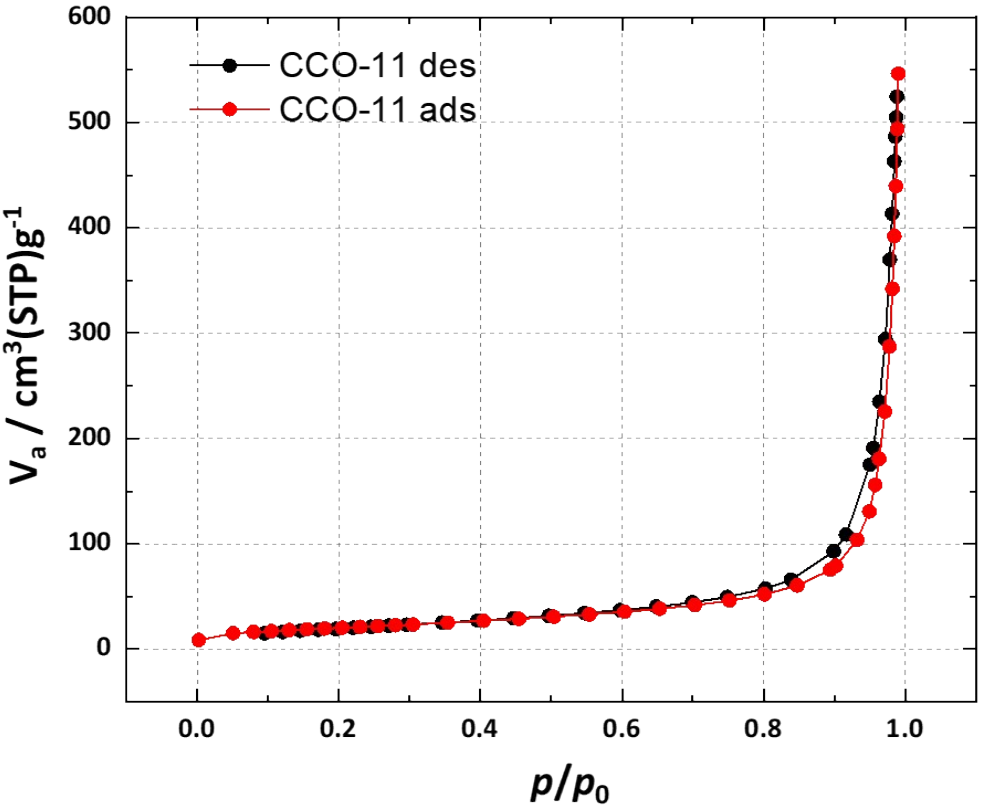

Fig. S11. Nitrogen adsorption/desorption isotherm and the BET surface area analysis of CCO-11

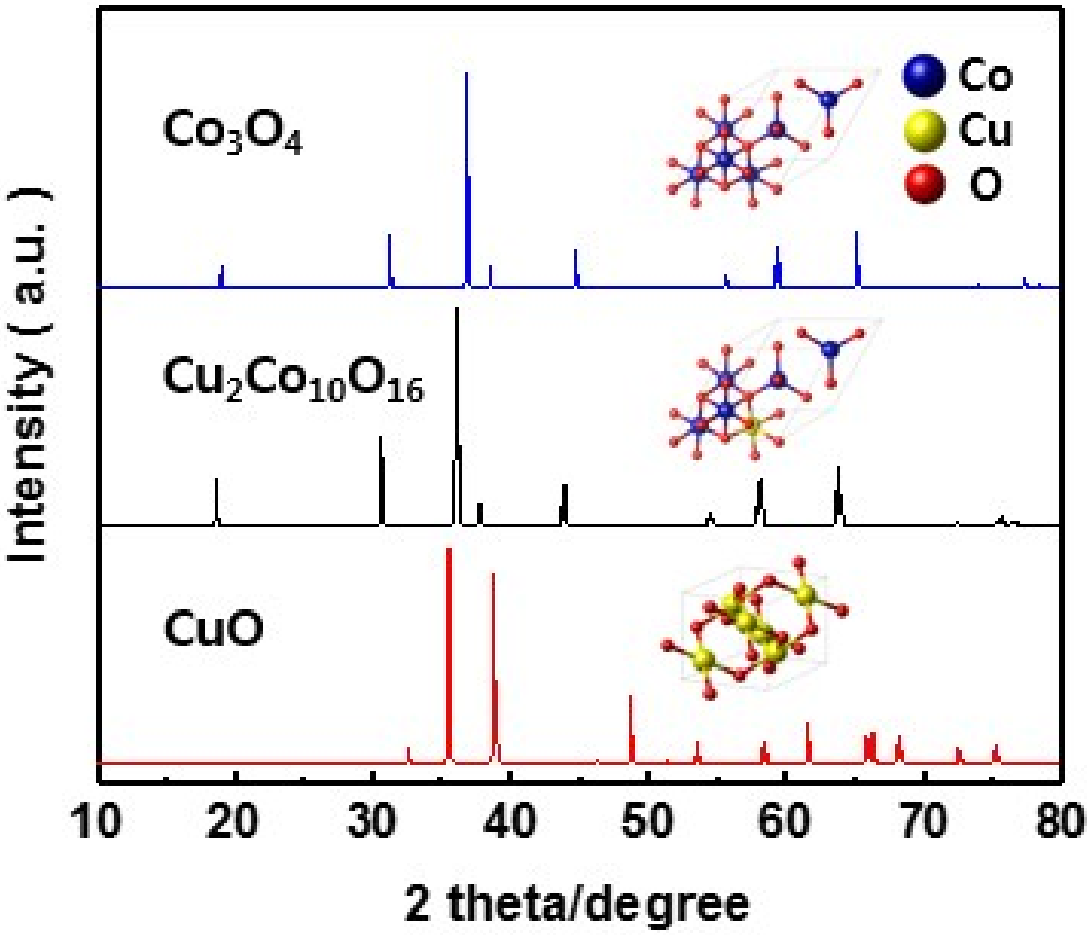

Fig. S12. X-ray diffraction (XRD) patterns of (blue line) for bulk Co_3O_4 in the symmetric group of Fd3m (ICSD #69374). (black line) $Cu_2Co_{10}O_{16}$ selected from the configurations in models considering the composition of Cu, Co and O in lattice having symmetric group of Fd-3mZ (ICSD #150806), and (red line) for bulk CuO in the symmetric group of C12/c1 (ICSD #69094), respectively.

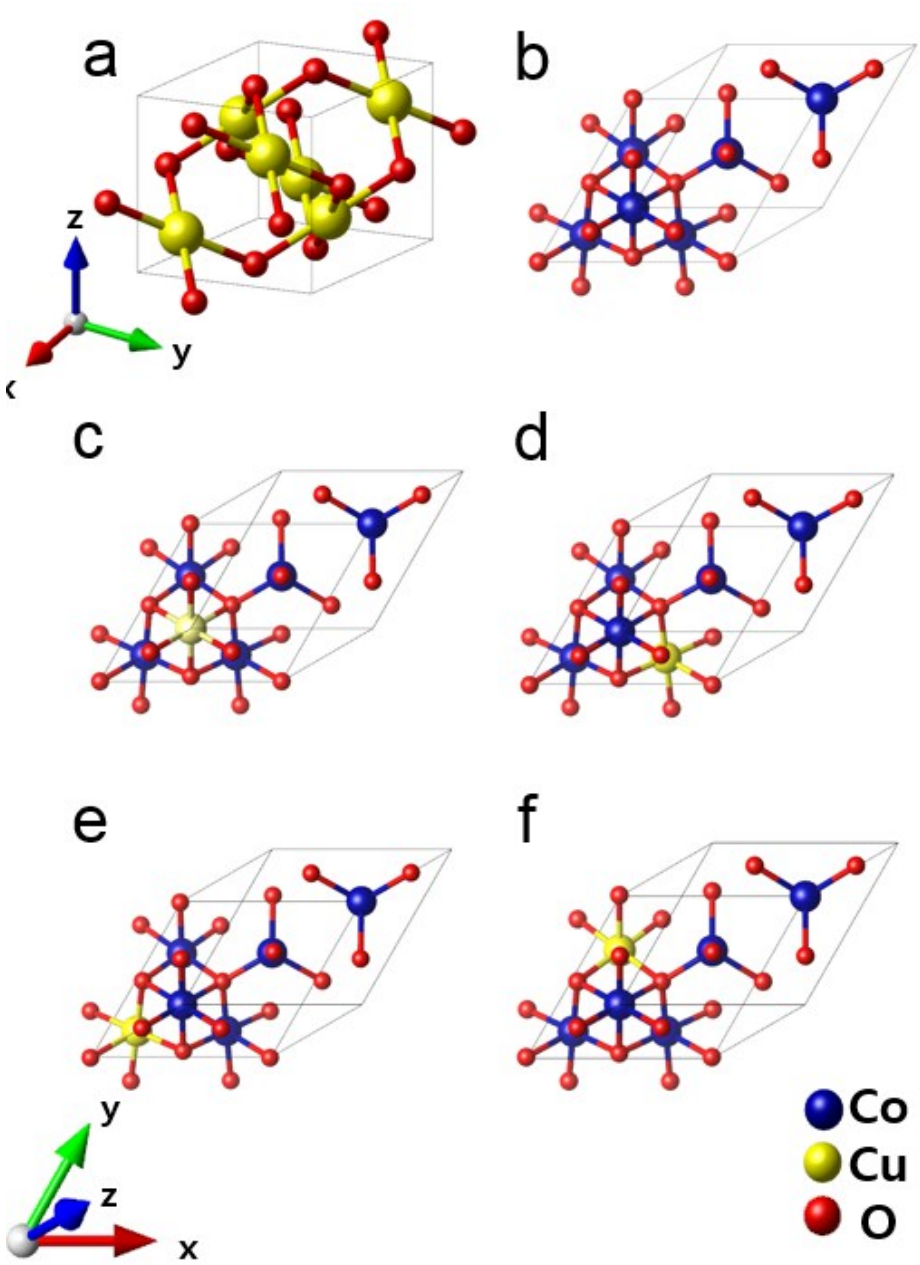

Fig. S13. Designed CuO in the symmetric group of C12/c1 (ICSD #69094), Co_3O_4 in the symmetric group of Fd3m (ICSD #28158) and $Cu_2Co_8O_{16}$ selected from the configurations in models considering the composition of Cu, Co, and O in lattice having a symmetric group of Fd-3mZ (ICSD #69374)

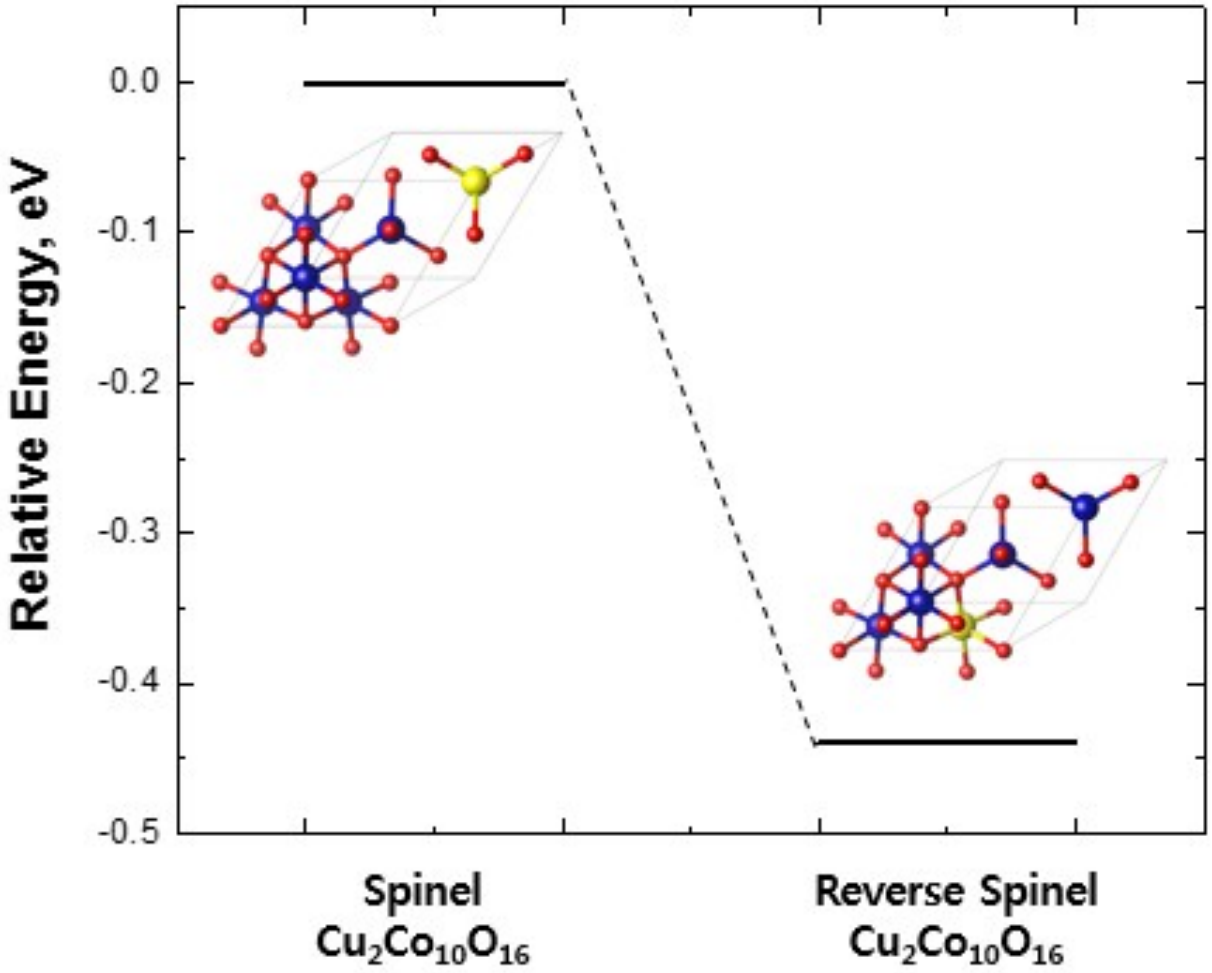

Fig. S14. Relative energy plot for the spinel and reverse spinel structures in $Cu_2Co_{10}O_{16}$.

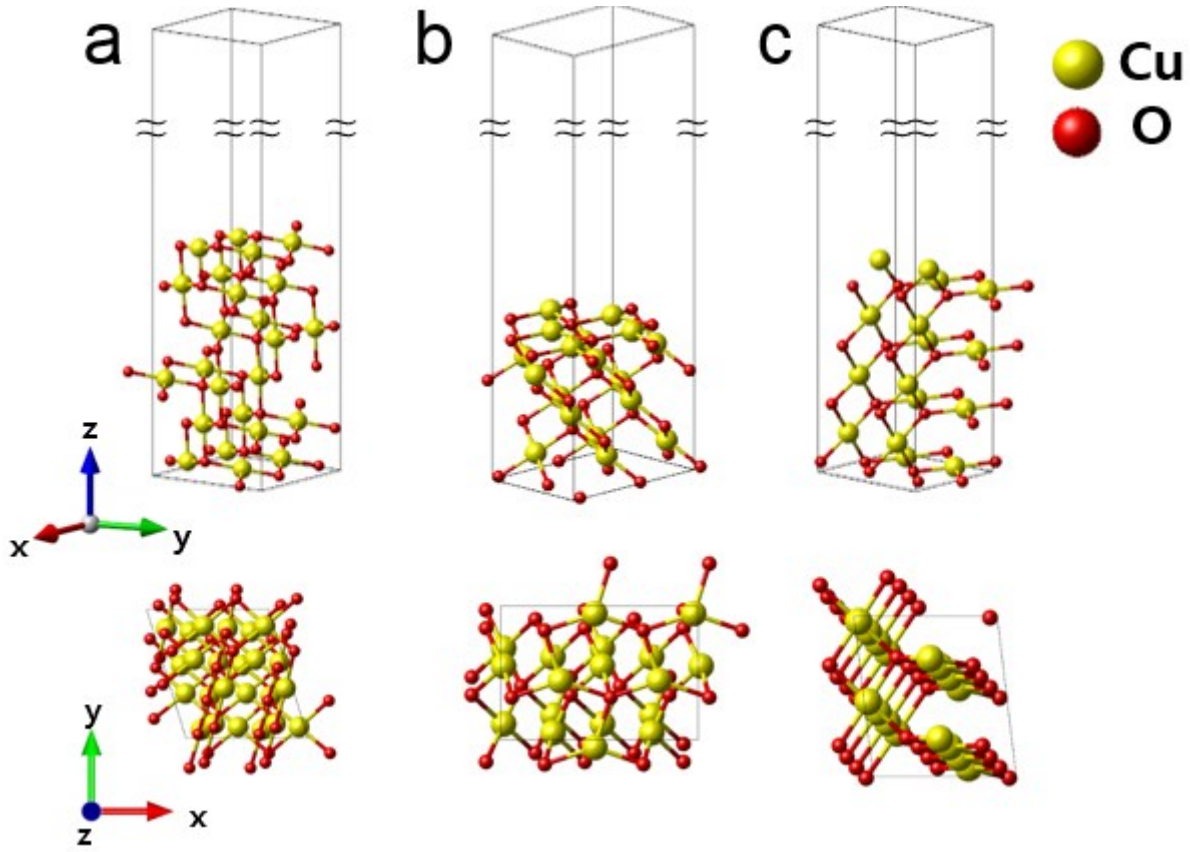

Fig. S15. (a) (001), (b) (110), and (c) (111) slab models of fully relaxed CuO. Based on the Z-coordination, bottom layers were fixed below 0.16, 0.12, and 0.16 for (001), (110), (111) of each slab model, respectively, from the bottom termination to be not included in the surface reaction. Rest atoms were fully relaxed.

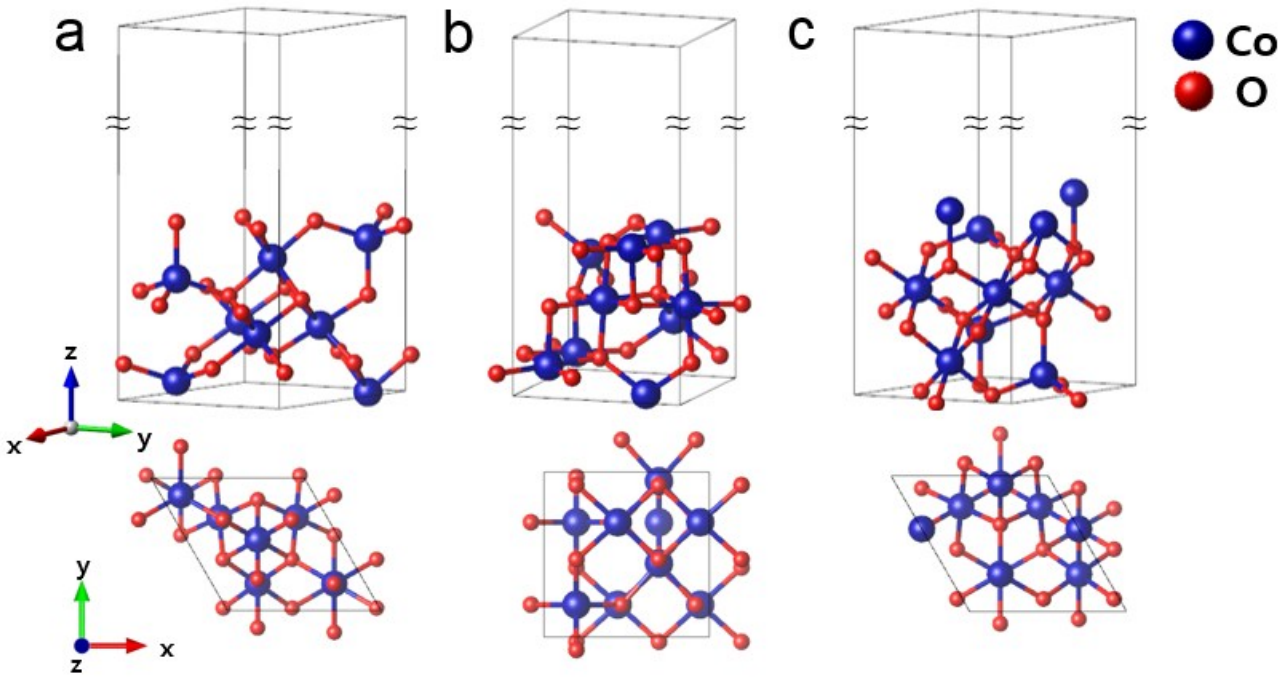

Fig. S16. (a) (001), (b) (110), and (c) (111) slab models of fully relaxed Co_3O_4. Based on the Z-coordination, bottom layers were fixed below 0.12, 0.12 and 0.15 for (001), (110), (111) of each slab model, respectively, from the bottom termination to be not included in the surface reaction. Rest atoms were fully relaxed.

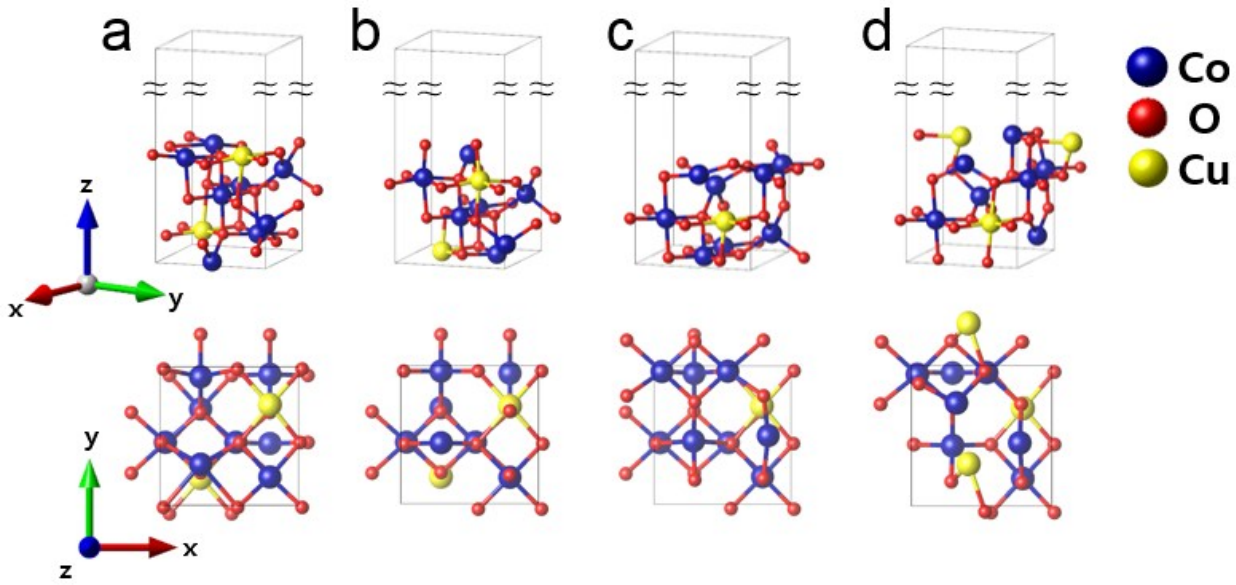

Fig. S 17. Designed slab models of four $Cu_2Co_{10}O_{16}$ (110) with different exposed surfaces.

References for Supplementary Information

(1) J. Bao, X. Zhang, B. Fan, J. Zhang, M. Zhou, W. Yang, X. Hu, H. Wang, B. Pan, Y. Xie, *Ang. Chem. Int. Ed.*, 2015, **54**, 7399-7404.

(2) W. Xu, F. Lyu, Y. Bai, A. Gao, J. Feng, Z. Cai, Y. Yin, *Nano Energy*, 2018, **43**, 110-116.

(3) H. Hu, B. Guan, B. Xia, X.W. Lou, *J. Am. Chem. Soc.*, 2018, **137**, 5590-5595.

(4) Y. Wang, T. Zhou, K. Jiang, P. Da, Z. Peng, J. Tang, B. Kong, W.B. Cai, Z. Yang, G. Zheng, *Adv. Energy Mater.*, 2014, **4**, 1400696.

(5) Z. Liang, Z. Huang, H. Yuan, Z. Yang, C. Zhang, Y. Xu, W. Zhang, H. Zheng, R. Cao, *Chem. Sci.*, 2018, **9**, 6961-6968.

(6) H.Y. Wang, Y.Y. Hsu, R. Chen, T.S. Chan, H.M. Chen, B. Liu, *Adv. Energy Mater.*, 2015, **5**, 1500091.

(7) L. Han, X.Y. Yu, X.W. Lou, *Adv. Mater.*,2016, **28**, 4601-4605.

(8) A.L. Strickler, M.a. Escudero-Escribano, T.F. Jaramillo, *Nano Lett.*, 2017, **17**, 6040-6046.

(9) X. Lu, Y.H. Ng, C. Zhao, *ChemSusChem*, 2014, **7**, 82-86.

(10) X. Wu, K. Scott, *J. Power Sources*, 2012, **214**, 124-129.

(11) Y.C. Cao, X. Wu, K. Scott, *Int. J. Hydrogen Energy*, 2012 , **37**, 9524-9528.

(12) C.C. Pavel, F. Cecconi, C. Emiliani, S. Santiccioli, A. Scaffidi, S. Catanorchi, M. Comotti, *Ang. Chem. Inter. Ed.*, 2014, **53**, 1378-1381.

(13) L. Xiao, S. Zhang, J. Pan, C.X. Yang, M.L. He, L. Zhuang, J.T. Lu, *Energy Environ. Sci.*, 2012, **5**, 7869-7871.

(14) X. Wu, K. Scott, *Int. J. Hydrogen Energy*, 2013, **38**, 3123-3129.

(15) T. Pandiarajan, L.J. Berchmans, S. Ravichandran, *Rsc Adv.*, 2015, **5**, 34100-34108.

(16) X. Wu, K. Scott, *J. Mater. Chem.*, 2011, **21**, 12344-12351.

(17) Y. Leng, G. Chen, A.J. Mendoza, T.B. Tighe, M.A. Hickner, C.Y. Wang, *J. Am. Chem. Soc.*, 2012, **134**, 9054-9057.

(18) J.E. Park, S. Kim, O.-H. Kim, C.-Y. Ahn, M.-J. Kim, S.Y. Kang, T.I. Jeon, J.-G. Shim, D.W. Lee, J.H. Lee, Y.-H. Cho, Y.-E. Sung, *Nano Energy*, 2019, **58**, 158-166.

(19) M.K. Cho, H.Y. Park, H.J. Lee, H.J. Kim, A. Lim, D. Henkensmeier, S.J. Yoo, J.Y. Kim, S.Y. Lee, H.S. Park, J.H. Jang, *J. Power Sources*, 2018, **382**, 22-29.